

NONDESTRUCTIVE EVALUATION OF SUPERALLOY SPECIMENS WITH A THERMAL BARRIER COATING

J.H. Heida

National Aerospace Laboratory NLR, Amsterdam, The Netherlands

Abstract: This paper describes an investigation into the applicability of NDE techniques for the inspection of superalloy specimens with a thermal barrier coating (TBC), both in unloaded condition and during constant load exposure at high temperatures (creep). More specifically, the eddy current (ET) and ultrasonic (UT) techniques were investigated for the characterisation of the TBC, while the acoustic emission (AE) technique was examined for the monitoring of the degradation incurred in the material during creep. Both uncoated and TBC specimens of single crystal and directionally solidified material were used in the investigation.

The main conclusions of the investigation are:

- The ET technique can be effectively used in the measurement of the coating thickness. The phase and the length of the lift-off response give information about the thickness of the bond coat and top coat, respectively. Differences in the bond and top coat thickness of about 10 μm can be distinguished.
- The UT technique does not provide enough information about the thickness or the quality of the TBC.
- The AE technique can be effectively used during creep testing to monitor the evolution of the material degradation, particularly in the coating layer of the TBC specimens. A distinctly different AE response was observed in the TBC specimens when creep tested at a different temperature (750 to 950°C). A correlation between the number of AE events and the number of coating cracks was demonstrated.

Introduction: Industrial gas turbine (IGT) manufacturers have demanding targets for efficient and clean power generation. These targets require higher turbine inlet and blade/vane operating temperatures and therefore the use of single crystal (SX) superalloys is invariably necessary. Moreover, the greater the temperature advantage of a particular SX alloy, the less cooling air is required. The selection of a SX superalloy for use in an IGT blade/vane application is dependent on both its high temperature properties and its castability. SX superalloys offer very good mechanical properties that can, together with appropriate coatings and advances in cooling technology, enable the IGT manufacturers to achieve the operating conditions required for efficient and low emission power plant. Although the blades and vanes are now routinely coated for oxidation and corrosion protection, a thermal barrier coating (TBC) is believed to be essential to meet the demanding efficiency and emission targets. At the same time, however, it is essential that component production and engine maintenance costs do not increase at a disproportionate rate. The production costs are primarily associated with the purchase of the raw material, the casting and heat treating procedures. Maintenance costs are linked to the reliability of the blade/vane components, the frequency and type of inspection, and the intervals for their scheduled replacement (Ref. 1).

This paper describes an investigation into the applicability of NDE techniques for the inspection of CM186LC SX specimens with a thermal barrier coating (TBC), both in unloaded condition and during constant load exposure at high temperatures (creep). CM186LC SX is a Ni-based superalloy with addition of Rhenium (second-generation superalloy). The chemical composition of this material is given in Table 1. Besides SX material also directionally solidified (SD) material was used in the investigation.

C	Cr	Co	Mo	W	Al	Ti	Ta	Re	B	Zr	Hf	Fe	Ni
0.069	6.0	9.3	0.5	8.4	5.7	0.7	3.4	2.9	0.015	0.006	1.4	0.065	Balance

Table 1 Chemical composition of typical CM186 bar stock (wt pct)

Both uncoated and TBC specimens were used in the investigation. The TBC system deposited on the specimens consists of an oxidation-resistant PtAl bond coat (referred to as CN91) and a ceramic ($\text{ZrO}_2+6-8\% \text{Y}_2\text{O}_3$) top coat. The CN91 bond coat was applied using a Chemical Vapour Deposition (CVD) process resulting in a single phase structure of 50-75 μm thickness. The top coat was deposited using an electron beam physical vapour deposition process (EB-PVD) that gives a 'distinctive' columnar structure, typically 100-150 μm thick, see Figure 1(a). All

specimens were coated at Chromalloy (UK). Following destructive examination of selected coated specimens, it was found that the bond and top coat layers often varied in thickness (see also Fig. 5). Further, in some specimens the bond coat displayed an unusual second ‘white’ phase (probably intermetallic phases including PtAl and Pt₂Al) close to the ceramic/bond coat interface, see Figure 1(b). The differences occurred due to the production in different batches.

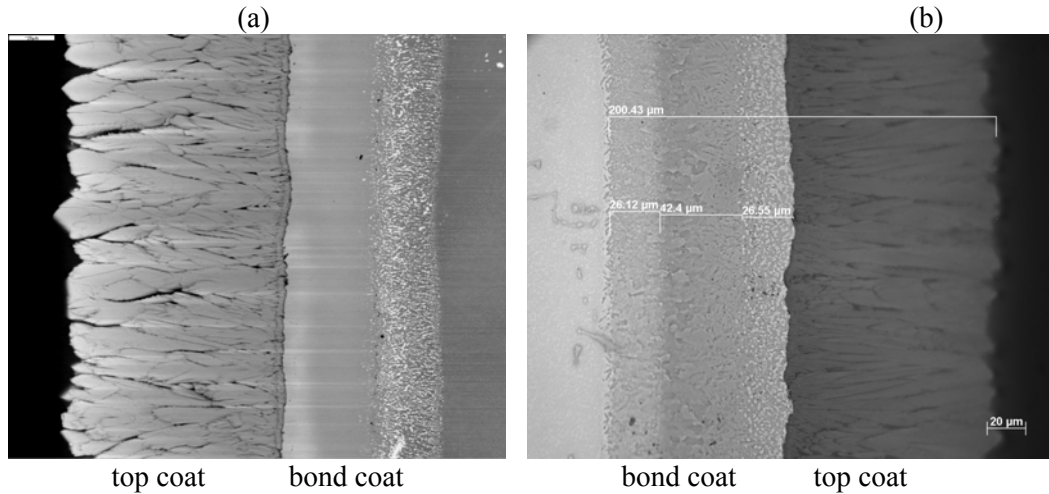


Fig. 1 (a) Typical CN91 bond coat coat (50-75 µm thick) with columnar EB-PVD top coat. (b) CN91 bond coat of increased thickness (95-105 µm), showing ‘white’ phase at the ceramic/bond coat interface

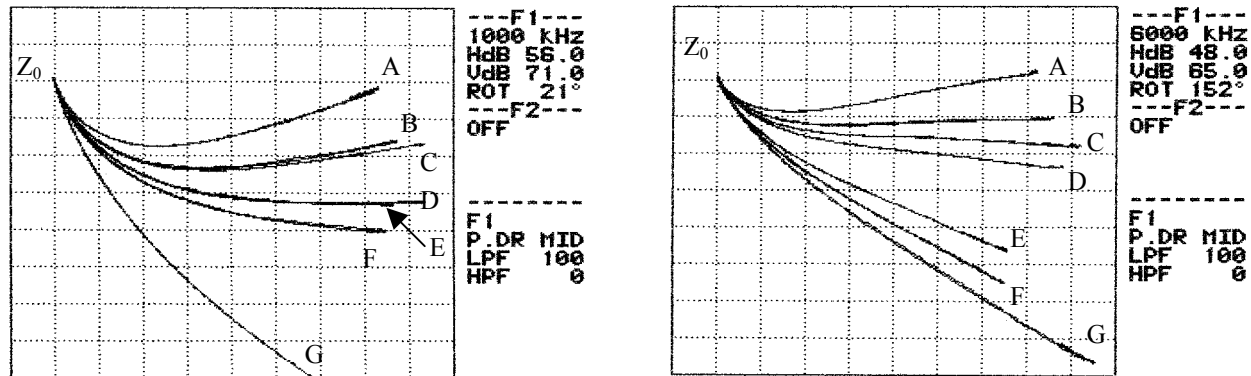
The investigation was carried out within the framework of the COST 522 programme on “Ultra Efficient, Low Emission Power Plant” (1999-2003). COST is the acronym for European Co-operation in the field of Scientific and Technical Research. Participants in COST 522 included a significant number of R&D centres and academic institutions such as the Technology Centres of ALSTOM and Powergen (UK), Howmet Ltd (UK), Imperial College and QinetiQ (UK), NTUA (Greece), FZJ and BAM (Germany), CNR-IENI and CESI (Italy), IPM (Czech Republic), AGH-UST (Poland), TUD (Denmark), TUK (Slovak Republic) and NLR (Netherlands).

Results: The ET and UT techniques were investigated for the characterisation of the TBC, while the AE technique was examined for the monitoring of the coating degradation incurred in the material during creep. The results of the investigation are given in Reference 2 and summarised in this paper.

Eddy current inspection (ET)

High-frequency ET lift-off measurements were performed on all available specimens with Nortec-19e^{II} equipment and a Nortec reflection shielded absolute probe (probe tip diameter 3 mm). The measurement implies the placing of the probe on the test part while recording the resulting coil impedance change (amplitude and phase angle). This impedance change is caused by the change in magnetic coupling between coil and test part. It is known that such measurements can be used for the determination of coating thickness differences (Ref. 3).

First, the *influence of test frequency* on the lift-off measurements of a number of flat specimens was investigated, see Figure 2. A frequency range of 1–6 MHz was applied to obtain a depth of ET penetration of less than 1 mm in the specimens. This high frequency is necessary due to the relatively low conductivity of superalloys (about 1% IACS). For these materials the standard depth of penetration is about 0.7 mm at 1 MHz and 0.3 mm at 6 MHz. The frequency of 6 MHz is the upper limit of the frequency range of the Nortec-19e^{II} test equipment.

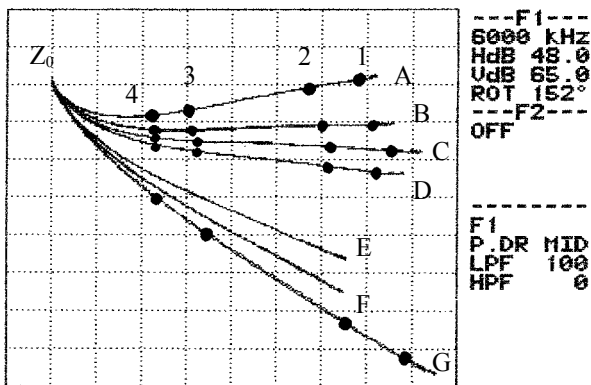


A: Ti-6Al-4V (1.0% IACS), B: CM186 SX uncoated, C: CM186 SX with PtAl bond coat
 D: Inconel 718 (1.4% IACS), E and F: CM186 SX TBC, G: Stainless steel (2.5% IACS)
 Z_0 : Coil impedance in air

Fig. 2 Impedance plots of ET lift-off responses of flat specimens. Influence of test frequency (1 and 6 MHz)

Figure 2 shows that there is a good separation of the lift-off signal between materials of different conductivity, with a sensitivity of about 0.1% IACS. The lift-off line of uncoated CM186 SX (line B) is located approximately between the lift-off lines of Ti-6Al-4V and Inconel 718. Hence, the conductivity of CM186 SX can be estimated at about 1.2% IACS. Figure 2 further shows a good separation between uncoated (line B) and TBC CM186 material (lines E and F), due to the influence of the bond coat. This influence is such that the lift-off line shifts towards material with higher conductivity, due to the relatively high conductivity of the constitutive elements Ni, Pt and Al in the bond coat. The lift-off line separation increases with increasing ET test frequency. This can be expected due to the smaller penetration depth of the eddy currents at a higher test frequency. The frequency of 6 MHz (penetration depth about 0.25 mm) provided the best separation between the lift-off lines of uncoated and coated material. Another observation from Figure 2 is that the lift-off line of CM186 SX provided with a PtAl bond coat only (line C) is well separated from the lift-off lines of TBC CM186 material (lines E and F). This lift-off separation is due to *differences in bond coat thickness*, as the bond coat thickness is 50-60 μm for the line C specimen and 95-105 μm for the line E/F specimen.

To illustrate the *influence of a non-conductive top coat* on the lift-off line, non-conductive foils of different thickness (24, 68, 251 and 355 μm) were placed on the available flat specimens and the resulting lift-off lines were recorded, see Figure 3. The bullets (1 to 4) indicate the end of the lift-off lines for placement of a specific foil thickness on the base material. Figure 3 shows the expected behaviour of a true non-conductive layer placed on a conductive base material: an increase in the thickness of the non-conductive layer results in a shift along the same lift-off line towards the air point in the impedance plane (Z_0 : ET probe in air). Thickness differences of about 10 μm can be distinguished. No phase change of the lift-off line is expected and Figure 3 confirms this.

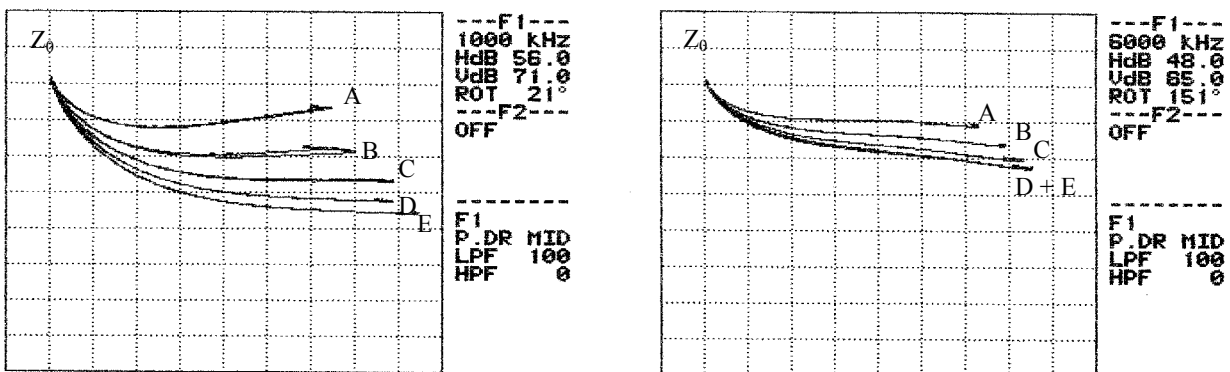


Flat specimens
 A: Ti-6Al-4V (1.0% IACS)
 B: CM186 SX uncoated
 C: CM186 SX + PtAl bond coat
 D: Inconel 718 (1.4% IACS)
 E: CM186 SX TBC
 F: CM186 SX TBC
 G: Stainless steel (2.5% IACS)

Non-conductive top coat thickness
 24 μm (1), 68 μm (2), 251 μm (3) and
 355 μm (4)

Fig. 3 Impedance plot of ET lift-off responses (frequency 6 MHz). Influence of thickness of a non-conductive foil on base material

Figure 4 shows the *influence of diameter* when recording the lift-off responses of test bars of different diameter in comparison with flat material. Because of material availability, uncoated Inconel 718 specimens were used. The figure shows that there is a distinct separation between the lift-off responses, because of a different magnetic coupling between ET probe and test part. This difference is caused by a geometrical factor and, therefore, is undesirable for in-service applications. As can be expected, an increase in the bar diameter results in a lift-off line located more closely to the one for flat material. The higher frequency of 6 MHz results in less separation of the different lift-off lines, when compared to the frequency of 1 MHz, due to the inherent smaller penetration depth (smaller field of ET influence). Figure 4 shows that the lift-off line of a bar with diameter 25.4

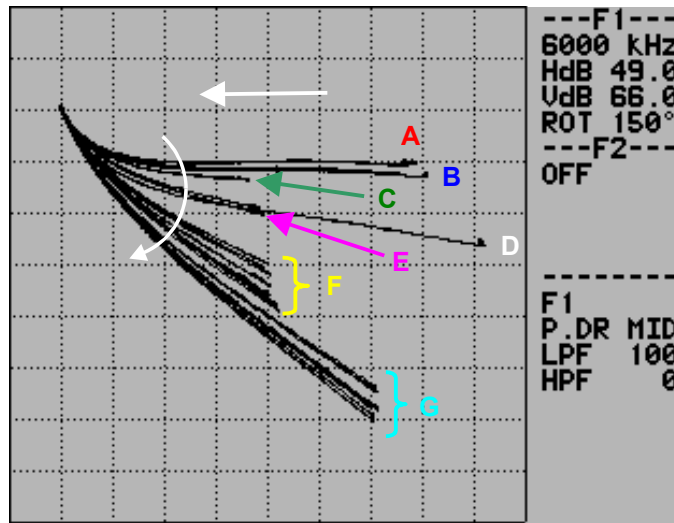


A: \varnothing 4.8 mm, B: \varnothing 8.0 mm, C: \varnothing 12.8 mm, D: \varnothing 25.4 mm, E: flat specimen, Z_0 : impedance in air

Fig. 4 Impedance plots of ET lift-off responses (frequency 1 and 6 MHz). Influence of different diameter (\varnothing) of uncoated Inconel 718 bars

mm at the frequency of 6 MHz already coincides with the line for flat material.

It can be concluded that 6 MHz is the *optimum ET test frequency* (within the limitations of the test equipment), because it results in a better separation of the lift-off signal for different materials and for uncoated/coated specimens, and less separation of the lift-off signal for flat/cylindrical specimens (i.e. smaller sensitivity to curvature changes).



Lift-off line	Specimen details	Creep tested	Bond coat thickness [μm]	thickness [μm]
	SX hollow creep specimens (2x)	--	None	None
B	SX hollow creep specimens (3x)	850-950°C	None	None
B	DS hollow creep specimen	--	None	None
C	DS hollow creep specimen	--	40 – 50	230 – 235
C	DS hollow creep specimen	950°C	40 – 50	190 – 200
D	SX solid bar, $\text{\O} 19 \text{ mm}$	--	50 – 60	None
E	SX hollow creep specimen	950°C	Not measurable	195 – 210
F	SX hollow creep specimen	--	65 – 87	190 – 195
G	SX solid bar with flat regions	--	95 – 105	105 – 115

Fig.5 Summary of the lift-off ET responses to a varying thickness of the bond coat and ceramic top coat in DS and SX CM186LC specimens. The circular arrow indicates the direction of increasing phase difference as a result of an increasing bond coat thickness. The white horizontal arrow points to the direction of a decreasing length in the lift-off response as a result of increasing top coat thickness

The systematic measurement of the lift-off responses in the available TBC CM186 specimens, coupled with subsequent visual measurement of the bond coat and top coat thickness in each specimen, has enabled an extensive evaluation of the eddy current technique, with the main lift-off responses summarised in Figure 5. The two main conclusions are the following:

- The phase of the lift-off response gives relevant information about the thickness of the bond coat. Examples of this can be found in Figure 5 when comparing the lift-off lines C, D, F and G. These correspond to specimens with an increasing bond coat thickness, as the tabulated data in Figure 5 confirm. The lift-off lines grouped under the letter F represent the ET responses at different locations along the periphery of a tubular specimen where the bond coat thickness was found to vary. The increasing phase shift, in the direction of the yellow circular arrow, corresponds to an increasing bond coat thickness, as visual (destructive) examination of this specimen has shown. The same response was obtained for the solid bar with flat sections, as shown by the lift-off lines grouped under G.
- The length of the lift-off response gives relevant information about the thickness of the top coat. Examples of this can be found in Figure 5 when comparing the lift-off lines of uncoated and TBC specimens, A, B and C respectively (although in the latter case the two lift-off lines overlap and hence the decrease in length due to the top coat thickness difference of 40 μm cannot be seen). The lines E, F and G exhibit both a phase

shift and a decrease in length, which is in agreement with the top coat thickness as the tabulated data in Figure 5 confirm.

The above results imply that, following careful calibration, the ET technique can be effectively used in the measurement of the coating thickness and that differences in the bond and top coat thickness of about 10 μm can be distinguished. The results in Figure 5 also suggest that the ET technique can probably be used for the monitoring of the coating degradation, as the comparison of the lift-off lines F and E from untested and tested TBC specimens shows (there are only small differences in the uncoated specimens, see lines A and B).

Ultrasonic inspection (UT)

UT pulse-echo measurements were performed in immersion using a Sonic-138 flaw scope, a LeCroy Waverunner LT342 and a number of focused transducers with a test frequency in the range of 5–34 MHz. Both solid (with circular and flat sections) and hollow specimens of uncoated and TBC CM186 SX material were inspected. However, it was found that because the thickness of the coating was too small, the coating interface did not introduce a substantial time difference in the time domain (i.e. the surface reflection signal was the same in uncoated and TBC specimens), or yield quantifiable differences in the frequency domain. It was therefore concluded that the UT technique does not provide enough information about the thickness or the quality of the TBC.

Acoustic emission (AE)

The AE technique was used to monitor the initiation and accumulation of damage in uncoated and TBC tubular specimens subjected to constant loads at three testing temperatures, 750, 850 and 950°C. The creep tests were performed in a creep bank of Applied Test Systems Inc., provided with a split furnace with side-entry extensometer cutout. An overview of the test set-up is given in Figure 6.



Fig. 6 Test set-up with the creep bank (with split furnace), AE equipment and the position of the AE sensors

AE inspections were carried out with a four-channel DiSP system of Physical Acoustics Corporation. Three channels were used for AE recording, one wideband 0-800 kHz sensor (WD) with a separate PAC 2/4/6 preamplifier and two resonant 150 kHz sensors with integrated preamplifier (R15I). Because of the temperature in the furnace (range 750-950°C), the sensors were mounted outside the furnace on the specimen clamping, see Figure 6. The upper two sensors are the actual measuring sensors; the lower one (R15I sensor) is acting as guard sensor to disregard any noise signals from the creep bank. Calibration of inspection was performed by checking the consistency of AE activity from lead-pencil breaks at different locations.

A distinctly different AE response (threshold 35 dB) was obtained in the uncoated and TBC specimens, see Table 2. The former showed a low level of AE activity during the creep test with, generally, a significant increase in the

number of AE events towards the later stages of the test. This is likely to be related to crack initiation and propagation from carbides and micropores, which is expected to take place during tertiary creep (Ref. 1).

Specimen TB coated	Temp [°C]	Stress [MPa]	Time to failure [hrs]	Creep strain [%]	Number of AE events
No	950	160	2028	13.0	60
Yes	950	160	2138	19.2	549
No	850	320	3660	~ 24	122
Yes	850	320	2641	21.1	2776
Yes	750	560	3669	7.9	8755

Table 2 Creep test and AE data of hollow tubular CM186 SX specimens

The AE response of the TBC specimens exhibited a significantly greater number of events (mainly in the 35-60 dB range) due to cracking in the coating layer (top coat). In addition, there was a different AE response of the specimens tested, according to the applied temperature, see e.g. Figures 7 and 8.

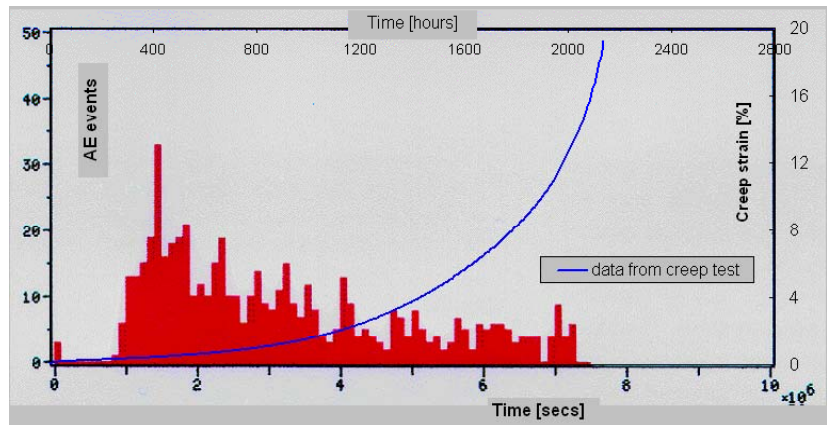


Fig. 7 AE events during the creep testing of a hollow TBC tubular CM186 SX specimen at 950°C and 160 MPa. The blue curve traces the recorded creep data points

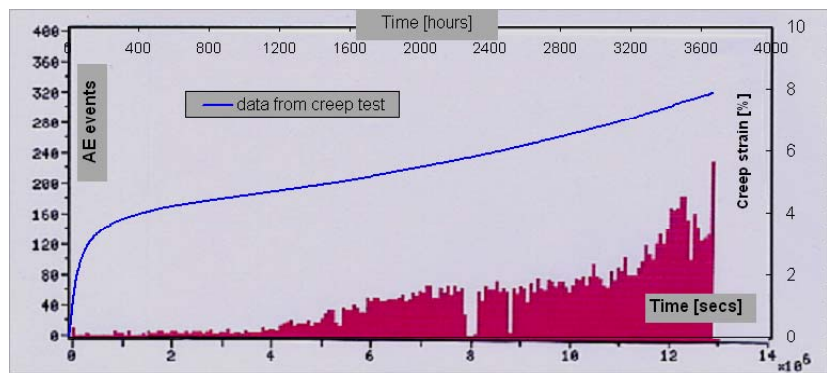


Fig. 8 AE events during the creep testing of a hollow TBC tubular CM186 SX specimen at 750°C and 560 MPa. The blue curve traces the recorded creep data points

At 950°C, due to the higher sintering rate there was a high AE activity in the first half of the test, well before the creep strain reached about 2% (Ref. 2). Sintering causes a densification of the ceramic layer (cross-linking of the columnar structure) and a much coarser microstructure within the columns, leading to a reduced strain tolerance of the top coat. At 850°C the AE events occurred toward the end of the test once the creep strain exceeded around 12%

(about 80% of the creep life), since the sintering of the TBC occurs at a lower rate. The total number of AE events, however, was considerably higher than at 950°C (Table 2). Finally, at 750°C, cracking in the coating started early as the creep strains quickly build-up during the primary stage, see Figure 8 noting the different scale in the ‘AE events’ axis in comparison to Figure 7. The cracking activity increased, however, significantly at creep strains between 4-5%. The total number of AE events was again much higher than with the creep tests at the higher temperatures. These remarks correlate well (qualitatively) with the cracking behaviour visually observed following sectioning of the specimens, see Figure 9. In conclusion, the AE technique can be effectively used during creep testing to monitor the evolution of the material degradation, particularly in the coating layer of the TBC specimens.

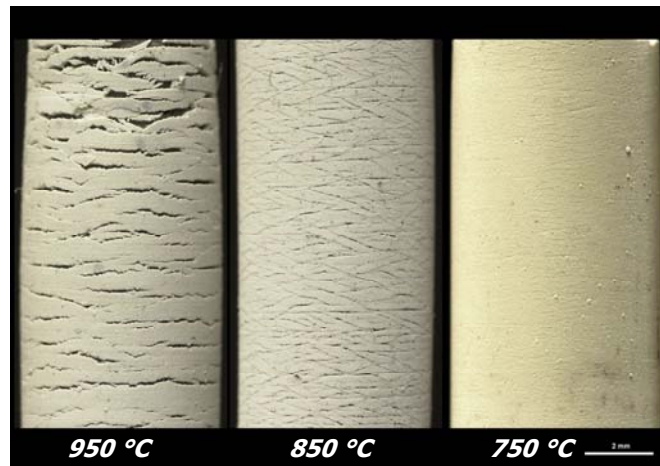


Fig. 9 Crack distribution in the TBC system of tubular CM186 SX specimens following creep testing at 950, 850 and 750°C

Conclusions:

- The ET technique can be effectively used in the measurement of the TBC thickness. The phase and the length of the lift-off response give information about the thickness of the bond coat and top coat, respectively. Differences in the bond and top coat thickness of about 10 μm can be distinguished.
- The UT technique does not provide enough information about the thickness or the quality of the coating.
- The AE technique can be effectively used during creep testing to monitor the evolution of the material degradation, particularly in the coating layer of the TBC specimens. A distinctly different AE response was observed in the TBC specimens when creep tested at a different temperature (750-950°C). A correlation between the number of AE events and the number of coating cracks was demonstrated.

References:

1. Toullos, M., *The mechanical behaviour of a class of rhenium based SX superalloys for industrial gas turbine applications*, Materials for advanced power engineering 2002, Proceedings of the 7th Liège Conference, Part I, J. Lecomte-Beckers et al (editors), held 30 September – 1 October 2002, Liège, Belgium, pp. 5-22.
2. Heida, J.H., *Nondestructive evaluation of CM186 specimens with a thermal barrier coating*, NLR report CR-2003-311, Amsterdam, May 2003.
3. Burkhardt et al, G.L., *Nondestructive evaluation of high-temperature coatings for industrial gas turbines*, Proceedings of the 8th International Symposium on Superalloys, held September 22-26, 1996, Champion, Pennsylvania, USA, pp. 747-752.